Communication

Cooperative Loading and Release Behavior of a Metal-Organic Receptor

Quan Gan, Tanya K Ronson, David A. Vosburg, John D. Thoburn, and Jonathan R. Nitschke

Just Accepted

Cooperative Loading and Release Behavior of a Metal-Organic Receptor

Quan Gan,[†] Tanya K. Ronson,[†] David A. Vosburg,[‡] John D. Thoburn,[§] and Jonathan R. Nitschke*,[†]

[†]Department of Chemistry, University of Cambridge, Lensfield Road, Cambridge CB2 1EW, United Kingdom

[‡]Department of Chemistry, Harvey Mudd College, 301 Platt Boulevard, Claremont, CA 91711, United States

[§]Department of Chemistry, Randolph-Macon College, Ashland, VA 23005, United States

Supporting Information Placeholder

ABSTRACT: In order to design artificial chemical systems that are capable of achieving complex functions, it is useful to design synthetic receptors that mimic their biological counterparts. Biological functions are underpinned by properties that include specific binding with high affinity and selectivity, cooperativity, and release triggered by external stimuli. Here we show that a metal-organic receptor constructed through subcomponent self-assembly can selectively and cooperatively load and release oxocarbon anions. The flexible coordination spheres of its cadmium(II) centers allow the receptor to dynamically adjust its structure upon exchanging two oxocarbon anions for four triflate or triflimide counterions, resulting in strong cooperativity and very tight binding, with an apparent association constant for $C_5O_5^{2-}$ of 5×10^{10} M^{-1}. Substituting the cadmium(II) ions for copper(I) by switching solvent prompted a structural reorganization and release of the oxocarbon anions. Its cooperative behavior allows the receptor to carry a greater payload than would be possible in a non-cooperative analogue.

The cooperative binding and release of substances in response to external stimuli is a key feature of metabolic and signaling functions in biological systems.[1] A canonical example is the dioxygen-transport protein hemoglobin, where dioxygen binding at one of the four sites increases the oxygen affinity of the other sites, resulting in efficient delivery of oxygen from respiratory organs to tissues where it is needed.[2] This cooperative behavior enables hemoglobin to deliver 1.7 times more oxygen than would be possible if the binding sites were non-cooperative.[3] The cooperative loading phenomenon in natural biomacromolecules has inspired the study of smaller synthetic analogues, both to better understand the mechanisms involved in natural systems and also to develop functional systems that may benefit from such binding interactions. Several groups have fruitfully investigated artificial guest catch-and-release molecular systems,[4] including both open architectures and closed capsules, as well as demonstrating artificial cooperative binding behavior.[5] The present work builds upon these foundations by demonstrating a receptor that is capable of not only coopera-tive, selective uptake,[6] but also controlled, complete release under well-defined conditions.

Subcomponent **A**, based on a *pseudo*-fourfold-symmetric (cyclopentadienyl)(cyclobutadienyl) cobalt (CpCoCb) moiety, was designed and synthesized based on literature precedent for related molecules.[7] Four anilines provide four 'arms' to react with 2-formylpyridines, generating a tetrakis(bidentate) ligand. Meta-substituted anilines were chosen to bring the ligand arms close enough to form a sandwich structure through free rotation between the anilines and the *para*-phenylene rings (Figure 1). Symmetrical sandwich structure **1** formed during the reaction of **A** with Cd^{II} and 2-formylpyridine **B** in a 2 : 4 : 8 ratio in acetonitrile. NMR and ESI-MS spectra of **1** were consistent with the formation of a highly symmetric M_4L_2 assembly in quantitative yield (Figures S1-S4).
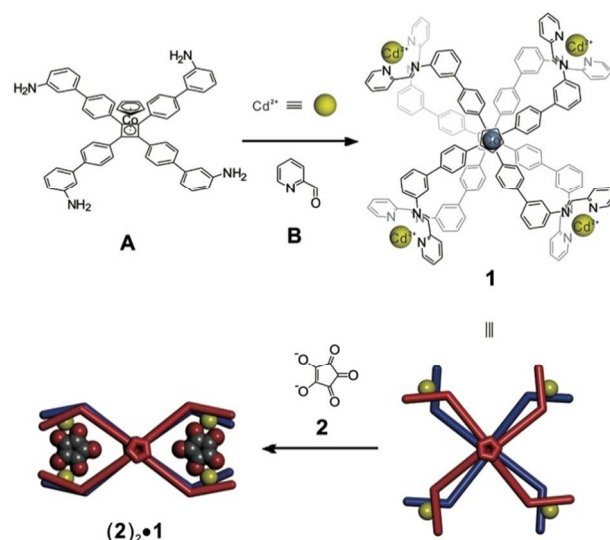

Figure 1. Synthesis and schematic representation of metal-organic receptor **1** and a (**2**)₂•**1** complex. The reaction of **A** (2 equiv.) and **B** (8 equiv.) with Cd^{2+} (4 equiv.) led to the formation of **1**. Addition of croconate anion (**2**) to **1** gave rise to a (**2**)₂•**1** complex.

The crystal structure of $\mathbf{1}\cdot(NTf_2)_8$ was consistent with the approximate D_4 symmetry observed in solution by NMR, in which two ligands are brought together by formation of coordination bonds, with the Cp rings on the exterior faces of the complex (Figure 2a,b). Each ligand coordinates to four Cd^{II} ions, with an average distance of 16.5 Å between adjacent metal centers. Each Cd^{II} is bound by a pyridyl-imine 'arm' from each ligand, leaving two free coordination sites that are occupied by acetonitrile or water to complete the octahedral coordination sphere of Cd^{II}.
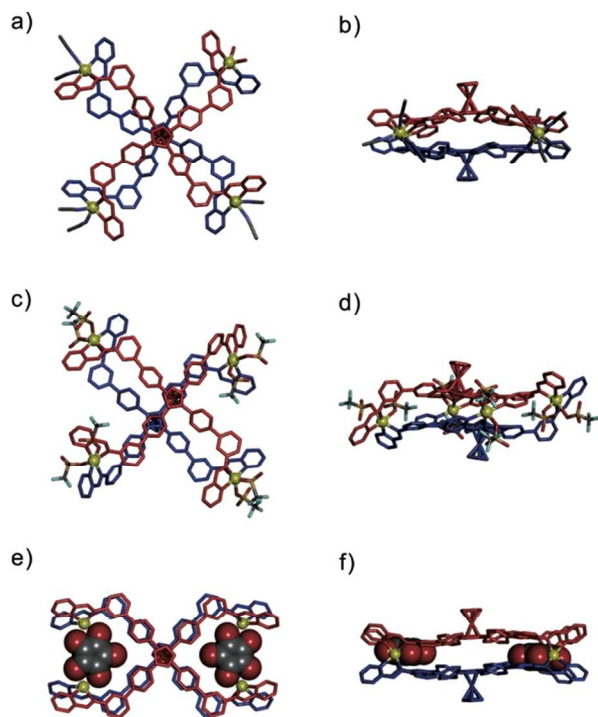

Figure 2. Top and side views of the crystal structures of $\mathbf{1}\cdot(NTf_2)_8$ (a & b), $\mathbf{1}\cdot(OTf)_8$ (c & d), and $(\mathbf{2})_2\cdot\mathbf{1}$ complex (e & f). Oxocarbon anions are shown as CPK representations (C gray, O red). Hydrogen atoms, uncoordinated counterions, solvent molecules and disorder have been omitted for clarity.[14]

The crystal structure of $\mathbf{1}\cdot(OTf)_8$ (Figure 2c,d), in contrast, possesses C_i symmetry, in which two opposing corners are similar to those of $\mathbf{1}\cdot(NTf_2)_8$, with the two pyridyl donors occupying *trans* coordination sites. The other two Cd^{II} centers adopt a less symmetric coordination geometry, having pyridyl donors *cis* to each other. The two central cyclobutadienyl rings, which are stacked atop each other in $\mathbf{1}\cdot(NTf_2)_8$ (centroid-centroid distance 4.5 Å), adopt a slipped, offset arrangement in $\mathbf{1}\cdot(OTf)_8$ (centroid-centroid distance 5.3 Å).

NMR measurements in solution provided evidence for the presence of two configurations of $\mathbf{1}$ for both the triflimide and triflate salts, with symmetries consistent with the two forms observed in the solid state. The triflimide salt was used in all of our solution studies due to the greater solubility of the resultant complexes in CD_3CN. At 278 K, NMR data were consistent with a D_4-symmetric structure, whereas a second set of signals appeared when the temperature was increased to 333 K (Figure S5). We infer the new species to be the C_i-symmetric conformation of $\mathbf{1}$, since it possesses twice as many resonances as the major D_4-symmetric species. Diffu-

sion-ordered ^1H NMR spectroscopy (DOSY) was also consistent with the two species having similar sizes (Figure S7). The enthalpy and entropy of transformation from the D_4 to C_i isomer in acetonitrile were determined using a van 't Hoff plot to be 6.7 kJ mol^{-1} and 4.5 J mol^{-1} K^{-1}, respectively (Figure S6). The positive values of both ΔH and ΔS illustrate that the D_4 symmetric conformation of receptor $\mathbf{1}$ is enthalpically preferred while the C_i conformation is favored entropically. We attribute the dynamic behavior of compound $\mathbf{1}$ to the flexible coordination sphere of the large Cd^{II} ions, which allows them to tolerate distorted coordination geometries.[8]

We hypothesized that $\mathbf{1}$ would be a suitable receptor for anions, whereby the weakly coordinated solvent or anions occupying the two vacant coordination sites at each Cd^{II} center would be displaced by more strongly coordinating anions. Furthermore, we envisaged that the dynamic reconfiguration of $\mathbf{1}$ might allow it to bind anions cooperatively *via* rearrangement of the coordination sphere of the metal centers upon addition of a suitable anion. NMR titration experiments of receptor $\mathbf{1}$ with the tetrabutylammonium salts of croconate ($C_5O_5^{2-}$, $\mathbf{2}$), squarate ($C_4O_4^{2-}$, $\mathbf{3}$) and rhodizonate ($C_6O_6^{2-}$, $\mathbf{4}$) were carried out. In all cases, complexation was inferred to occur, as new signals in the ^1H NMR spectra emerged, and free receptor signals decreased, consistent with slow exchange between complexed and uncomplexed states on the ^1H NMR time scale (Figures S8-S10). ESI mass spectra displayed ions corresponding to 1 : 2 complexes (Figures S16 and S17). During the titration process, we observed two new sets of peaks. One set of signals arose first but then decreased with further anion addition, while the other species gradually increased and remained following saturation; we therefore assigned these to the 1 : 1 and 1 : 2 complexes, respectively. DOSY NMR further showed comparable diffusion rates for the two complexes, suggesting that each ^1H NMR resonance belongs to the framework of an intact M_4L_2 receptor rather than to smaller fragments (Figure S13).

Further solution characterization of the complex was hindered by the ^1H NMR silence of the oxocarbon anions. The solid-state structure (Figure 2e,f), however, revealed the original M_4L_2 architecture with two bound molecules of $\mathbf{2}$. Each croconate anion is coordinated in a bridging bis-bidentate manner to two Cd^{II} centers, with an average Cd-O bond length of 2.3 Å. Each Cd^{II} center in $(\mathbf{2})_2\cdot\mathbf{1}$ is thus coordinated by two pyridyl-imine ligands and one croconate anion in a trigonal prismatic geometry, in contrast to the distorted octahedral coordination observed in the absence of the guest. Binding of the croconate anions thus induces a structural reorganization of the M_4L_2 architecture. The bridging anions bring pairs of Cd^{II} centers closer together, with the Cd···Cd distance shrinking from 16.5 Å to 7.4 Å, and the 'arms' of the receptor become eclipsed in order to reposition the free coordination sites to bind to the anions.

The squarate anion $\mathbf{3}$ was chosen for UV-Vis titration studies as the absorbances of both croconate and rhodizonate overlap with that of receptor $\mathbf{1}$. Nonlinear regression analysis[9] of the titration data (Figure S15) based on a 1 : 2 binding model gave macroscopic binding constants of $6.3 \pm 0.3 \times 10^4$ and $7.90 \pm 0.08 \times 10^5$ M^{-1}, respectively, for K_1 and K_2 in the 1 : 2 complexation of $\mathbf{1}$ with squarate anion $\mathbf{3}$ (binding constants averaged from three runs). The ratio of the corresponding microscopic binding constants, $K_{2\mu}/K_{1\mu} = 50$, clearly indicates the positive cooperative nature of this complexation and corresponds to a cooperative Gibbs free energy of −9.7 kJ

mol^{-1}. The measured apparent association constant (K_a) for **3** binding to **1** was calculated to be $5.2 \pm 1.1 \times 10^{10}$ M^{-1} (Figure S15), representing an affinity value that is a composite of the two binding events.

The observed high cooperativity may be interpreted to result from an induced-fit process during recognition:[10] when one oxocarbon anion docks into the receptor, displacing and exchanging for the less-well-bound counteranions, a conformational change is induced to fit the oxocarbon anion. The remaining binding site is thereby preorganized to have increased affinity for a second anion. The crystal structures provide insight as to how this process might occur. A key point is that the staggered 'arms' of the receptor become eclipsed following the binding of the first croconate. This eclipsing brings the other two arms of the complex together to bind the second croconate with high affinity.

The cooperative binding observed for squarate also occurred for croconate and rhodizonate. For each of these oxocarbon anions, the intermediate 1 : 1 complexes were never significantly populated during NMR titration experiments. Among these anions, croconate **2** bound most tightly to **1**, as inferred from NMR experiments where two anions were allowed to compete to bind (Figure S11); croconate was thus chosen for subsequent studies. The binding of receptor **1** with other anions was tested, but the cooperative binding behavior seen for **2**, **3**, and **4** was not observed in the cases of PF$_6^-$, BF$_4^-$, Br$^-$ or I$^-$ (Figure S12).

Having established cooperative loading of anions into **1**, we sought to release the anions completely without disturbing the overall structure. For this purpose the Cu$^{I}_4$L$_2$ analogue **5** of Cd$^{II}_4$L$_2$ receptor **1** was synthesized and studied (Figure S18). Unlike receptor **1**, each Cu^{I} metal center in complex **5** is fully saturated by two pyridyl-imine ligands, since Cu^{I} ions favor a tetrahedral coordination environment; the metal centers of **5** thus exhibited no tendency to coordinate anions. Upon the addition of excess croconate (4 equiv.) to **5**, no new peaks or shifts in the signals were observed in either DMSO-d_6 or CD$_3$CN by ^{1}H NMR (Figure S21). Further addition of croconate resulted in broadened signals and precipitation of **5** due to anion exchange.

When both Cu^{I} and Cd^{II} were present, we found that **1** and **5** interconverted upon variation of the solvent: complex **1** was preferred in acetonitrile, whereas **5** dominated in DMSO. As a result, **5** could be obtained by adding Cu^{I} to **1** in DMSO, and **5** could be converted into **1** *via* addition of Cd^{II} in acetonitrile. We infer the stronger solvation of free Cd^{II} by DMSO, and Cu^{I} by acetonitrile, to drive the solvent-dependent metal exchange that allows **1** and **5** to interconvert. The combination of different solvent stability and differential oxocarbon anion recognition ability allows us to envisage a cycle of loading and release of anions by solvent-mediated interconversion between **1** and **5**. The sequence of steps is shown in Figure 3: (i) To an acetonitrile solution of receptor **1** containing free Cu^{I} (4 equiv.) was added anion **2** (2.4 equiv.), leading to formation of the (2)$_2$•1 complex, *i.e.* anion loading. (ii) Addition of DMSO stimulated the replacement of the Cd^{II} ions of the complex with Cu^{I} ions, resulting in transformation of **1** into **5**, and thus release of the two equivalents of **2**. (iii) Addition of diethyl ether to the above solution followed by filtration of the precipitated **5** allowed its separation from the released **2** and Cd^{II} left in solution. (iv) Finally, complex **5** transformed back into receptor **1** following dissolution of the precipitate in acetonitrile

and the subsequent addition of Cd^{II} (4 equiv.). Each conversion step was monitored by ^{1}H NMR (Figure 4).

This cycle implements a strategy of cooperative catch and release of an anion in two different environments through altering the properties of the receptor upon addition of chemical stimuli. The considerable manipulation of compounds and solutions required by this strategy would be most worthwhile in the context of high-value extractions, as in the extraction of sulfate from nuclear waste.[11]
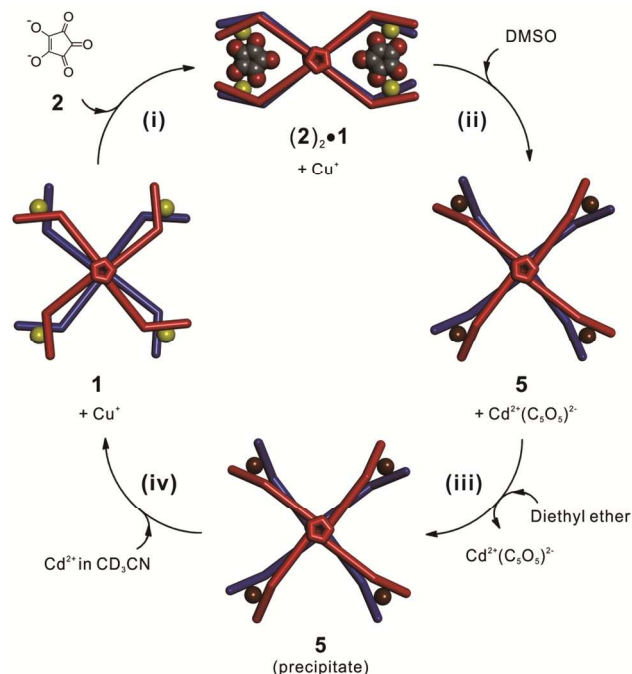

Figure 3. Schematic representation of loading and release of croconate with receptors **1** and **5** by switching the metal centers. **(i)** Trapping **2** as (2)$_2$•1. **(ii)** DMSO addition prompted metal exchange and release of anion **2**. **(iii)** Addition of diethyl ether gave solid complex **5**, with Cd^{2+}•2 in the filtrate. **(iv)** Redissolution of **5** in CD$_3$CN followed by addition of Cd^{2+} regenerated the initial state.

The addition of Cu^{I} to a solution of (2)$_2$•1 (Figure S22) resulted in its clean conversion to **5** and free **2**, without forming Cu^{I}-Cd^{II} hybrid structures. This observation suggests that both metal substitution and anion release are strongly cooperative. If the metal substitution process was not cooperative, partially exchanged receptor signals would be significant and would greatly complicate the NMR spectra. Interestingly, in the absence of oxocarbon anions, complicated spectra were observed during metal substitution (Figure S23), which we attribute to mixed-metal complexes.

The observed high-affinity cooperative catch and release behavior provides **1** with advantages in comparison with other artificial systems in which no cooperativity occurs.[5-12] At a concentration of 5.0×10^{-6} M, **1** would be half-saturated with **3** at an anion concentration of 8.0×10^{-6} M. In the absence of cooperativity, however, the hypothetical maximum amount of anion that could be loaded under the same conditions is 3.1×10^{-6} M. Thus, the cooperative binding behavior of the receptor enables it to deliver 1.6 times as much anion as it would if the sites were independent, a value comparable to the cooperative advantage enjoyed by hemoglobin in transporting oxygen.[4] Furthermore, **1** efficiently catches and releases anions at low concentrations within a narrow response region, where small changes in conditions lead to a

complete transformation between free and bound states. These features are of considerable benefit in the context of chemical sensors[12] or drug delivery systems.[13] Although we did not carry out studies on a sufficiently large scale to allow yield determination, NMR spectra did not show substantial impurity buildup (estimated < 5%) even after four turns around the cycle of Figure 3. This observation is consistent with an efficient strategy.
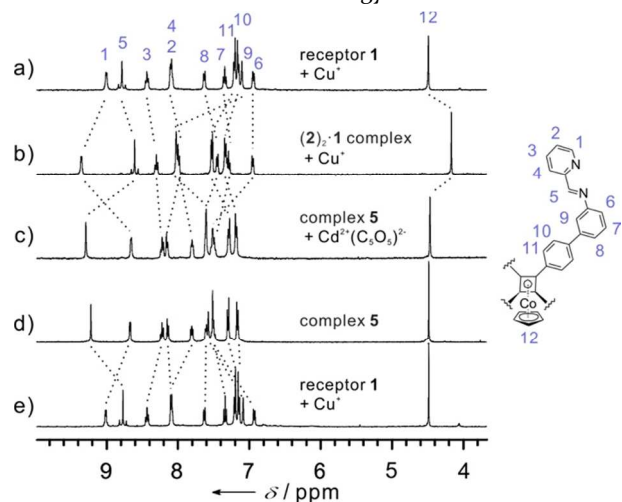

Figure 4. Partial ^{1}H NMR spectra (400 MHz, 298 K) of the catch and release of anions following the cycle of Figure 3. **a)** Receptor **1**•(NTf$_2$)$_8$ (0.25 mM) with Cu$^+$ (4 equiv.) in CD$_3$CN (500 μL); **b)** addition of **2** (2.4 equiv.) to solution **a**; **c)** addition of DMSO-d_6 (50 μL) to solution **b**; **d)** precipitate obtained from addition of diethyl ether to **c** following dissolution in CD3CN (500 μL); **e)** addition of Cd^{2+} (4 equiv.) to solution **d**.

In summary, we have shown how oxocarbon anions can be cooperatively loaded and released by regulating the properties of an artificial receptor. The binding of the first oxocarbon anion to receptor **1** increases the binding affinity of the second one, while both are released completely in the reverse process triggered by chemical stimuli (exchanging the solvent resulting in switching the metal centers). This system also illustrates induced-fit recognition behavior: the flexibility of the arms of the complex allows dynamic adjustment of its binding sites via rearrangement of the metal coordination geometry to cooperatively accommodate anions with high affinity.

ASSOCIATED CONTENT

Supporting Information

Full experimental procedures, NMR and ESI-MS spectra, X-ray crystallographic data including CIF files (also deposited with the Cambridge Crystallographic Data Centre as entries CCDC 1012306-1012309). This material is available free of charge via the Internet at http://pubs.acs.org.

AUTHOR INFORMATION

Corresponding Author

jrn34@cam.ac.uk

Notes

The authors declare no competing financial interests.

REFERENCES

(1) (a) Whitty, A. *Nat. Chem. Biol.* **2008**, *4*, 435. (b) Hunter, C. A.; Anderson, H. L. *Angew. Chem. Int. Ed.* **2009**, *48*, 7488.

(2) Perutz, M. F. *Quart. Rev. Biophys.* **1989**, *22*, 139.

(3) *Biochemistry;* Berg, J. M.; Tymoczko, J. L.; Stryer, L. Eds.; W. H. Freeman: New York, **2002**.

(4) (a) Han, M.; Michel, R.; He, B.; Chen, Y. S.; Stalke, D.; John, M.; Clever, G. H. *Angew. Chem. Int. Ed.* **2013**, *52*, 1319. (b) Kishi, N.; Akita, M.; Kamiya, M.; Hayashi, S.; Hsu, H.-F.; Yoshizawa, M. *J. Am. Chem. Soc.* **2013**, *135*, 12976. (c) Hiraoka, S.; Harano, K.; Shiro, M.; Shionoya, M. *Angew. Chem. Int. Ed.* **2005**, *44*, 2727. (d) Durola, F.; Rebek, J. *Angew. Chem. Int. Ed.* **2010**, *49*, 3189. (e) Pochorovski, I.; Ebert, M.-O.; Gisselbrecht, J.-P.; Boudon, C.; Schweizer, W. B.; Diederich, F. *J. Am. Chem. Soc.* **2012**, *134*, 14702. (f) Lewis, J. E.; Gavey, E. L.; Cameron, S. A.; Crowley, J. D. *Chem. Sci.* **2012**, *3*, 778. (g) Hua, Y.; Flood, A. H. *J. Am. Chem. Soc.* **2010**, *132*, 12838. (h) Schmitt, F. d. r.; Freudenreich, J.; Barry, N. P.; Juillerat-Jeanneret, L.; Süss-Fink, G.; Therrien, B. *J. Am. Chem. Soc.* **2011**, *134*, 754.

(5) (a) Pistner, A. J.; Lutterman, D. A.; Ghidiu, M. J.; Ma, Y.-Z.; Rosenthal, J. *J. Am. Chem. Soc.* **2013**, *135*, 6601. (b) Ikeda, M.; Tanida, T.; Takeuchi, M.; Shinkai, S. *Org. Lett.* **2000**, *2*, 1803. (c) Ikeda, T.; Hirata, O.; Takeuchi, M.; Shinkai, S. *J. Am. Chem. Soc.* **2006**, *128*, 16008. (d) Deutman, A. B.; Monnereau, C.; Moalin, M.; Coumans, R. G.; Veling, N.; Coenen, M.; Smits, J. M.; de Gelder, R.; Elemans, J. A.; Ercolani, G. *Proc. Natl. Acad. Sci. USA* **2009**, *106*, 10471. (e) Nabeshima, T.; Yoshihira, Y.; Saiki, T.; Akine, S.; Horn, E. *J. Am. Chem. Soc.* **2003**, *125*, 28. (f) Willans, C. E.; Anderson, K. M.; Potts, L. C.; Steed, J. W. *Org. Biomol. Chem.* **2009**, *7*, 2756. (g) Huang, W.-H.; Liu, S.; Zavalij, P. Y.; Isaacs, L. *J. Am. Chem. Soc.* **2006**, *128*, 14744. (h) Park, J. S.; Le Derf, F.; Bejger, C. M.; Lynch, V. M.; Sessler, J. L.; Nielsen, K. A.; Johnsen, C.; Jeppesen, J. O. *Chem. Eur. J.* **2010**, *16*, 848. (i) Sato, H.; Tashiro, K.; Shinmori, H.; Osuka, A.; Murata, Y.; Komatsu, K.; Aida, T. *J. Am. Chem. Soc.* **2005**, *127*, 13086. (j) Takezawa, H.; Murase, T.; Resnati, G.; Metrangolo, P.; Fujita, M. *J. Am. Chem. Soc.* **2014**, *136*, 1786. (k) Jiang, W.; Nowosinski, K.; Löw, N. L.; Dzyuba, E. V.; Klautzsch, F.; Schäfer, A.; Huuskonen, J.; Rissanen, K.; Schalley, C. A. *J. Am. Chem. Soc.* **2012**, *134*, 1860.

(6) (a) Kremer, C.; Lützen, A. *Chem. Eur. J.* **2013**, *19*, 6162. (b) Chakrabarty, R.; Mukherjee, P. S.; Stang, P. J. *Chem. Rev.* **2011**, *111*, 6810.

(7) Harrison, R. M.; Brotin, T.; Noll, B. C.; Michl, J. *Organometallics* **1997**, *16*, 3401.

(8) Meng, W.; Ronson, T. K.; Clegg, J. K.; Nitschke, J. R. *Angew. Chem. Int. Ed.* **2013**, *52*, 1017.

(9) Thordarson, P. *Chem. Soc. Rev.* **2011**, *40*, 1305.

(10) Koshland, D. E. Jr. *Angew. Chem. Int. Ed.* **1995**, *33*, 2375.

(11) (a) Custelcean, R.; Remy, P.; Bonnesen, P. V.; Jiang, D.-e.; Moyer, B. A. *Angew. Chem. Int. Ed.* **2008**, *47*, 1866. (b) Custelcean, R.; Bonnesen, P. V.; Duncan, N. C.; Zhang, X.; Watson, L. A.; Van Berkel, G.; Parson, W. B.; Hay, B. P. *J. Am. Chem. Soc.* **2012**, *134*, 8525.

(12) Vajpayee, V.; Song, Y. H.; Lee, M. H.; Kim, H.; Wang, M.; Stang, P. J.; Chi, K. W. *Chem. Eur. J.* **2011**, *17*, 7837.

(13) Su, X.; Aprahamian, I. *Chem. Soc. Rev.* **2014**, *43*, 1963.

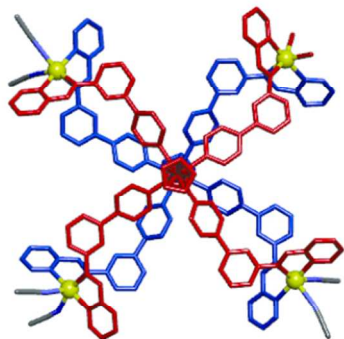(14) Coles, S. J.; Gale, P. A. *Chem. Sci.* **2012**, *3*, 683.
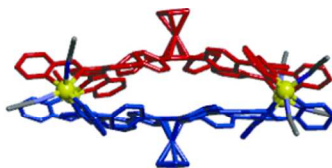
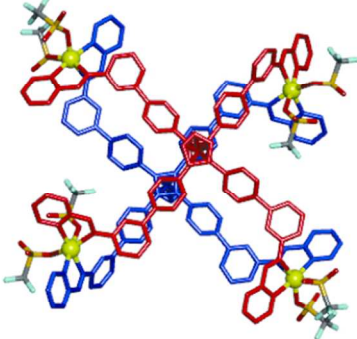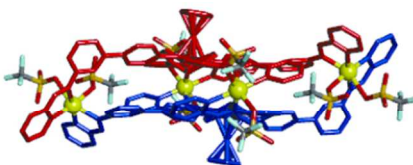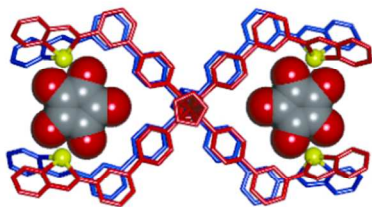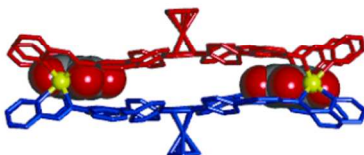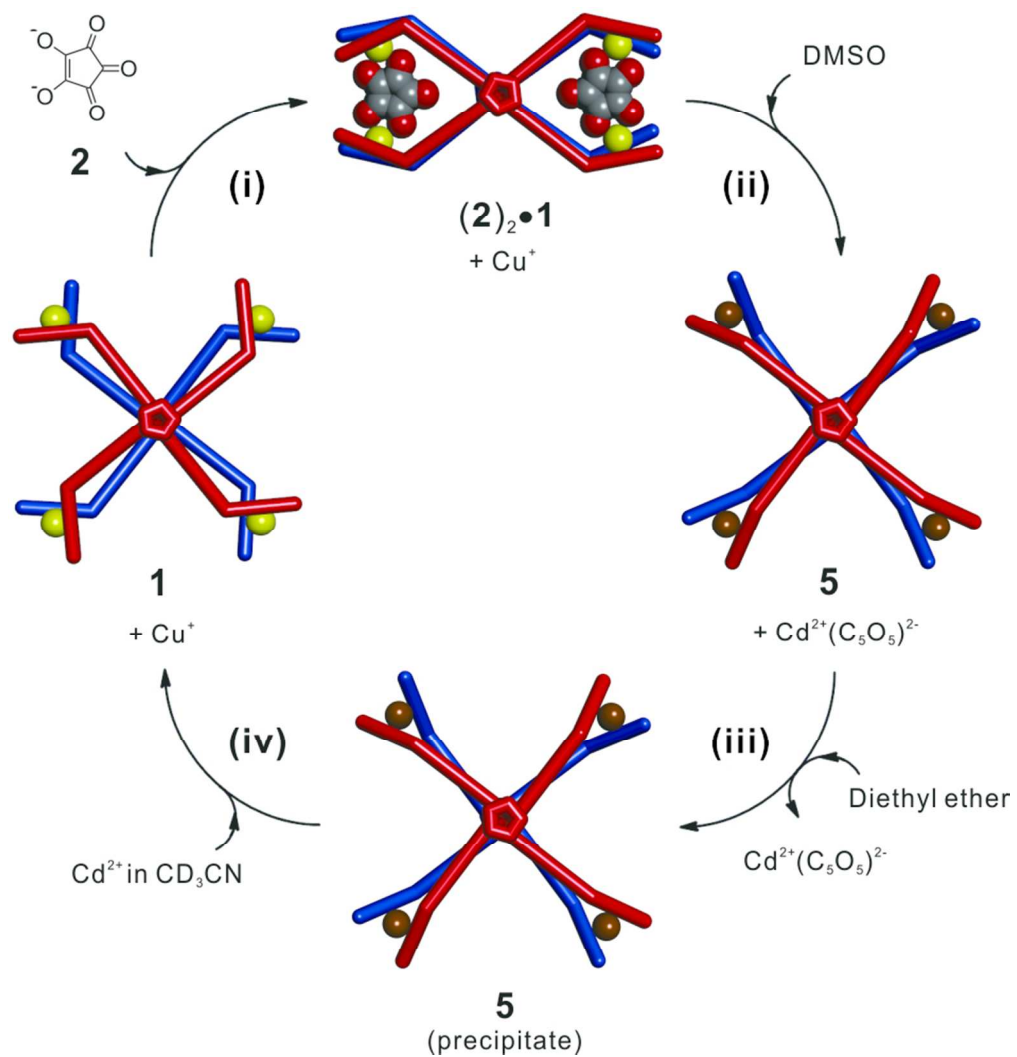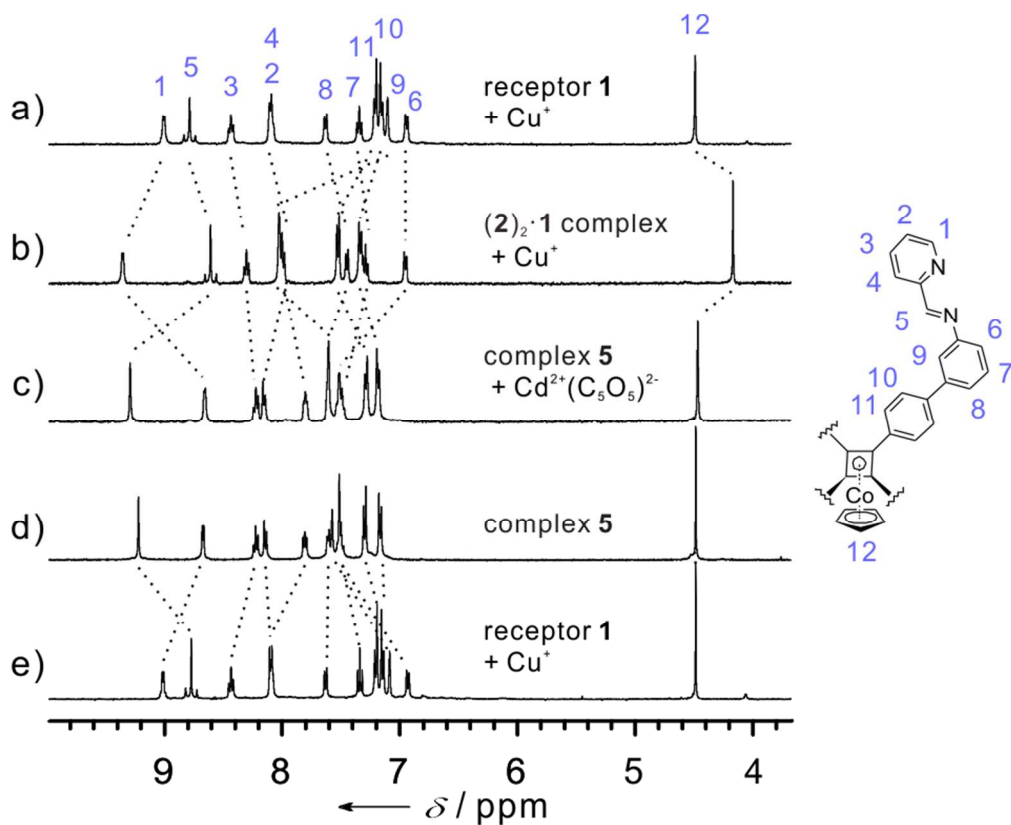Insert Table of Contents artwork here
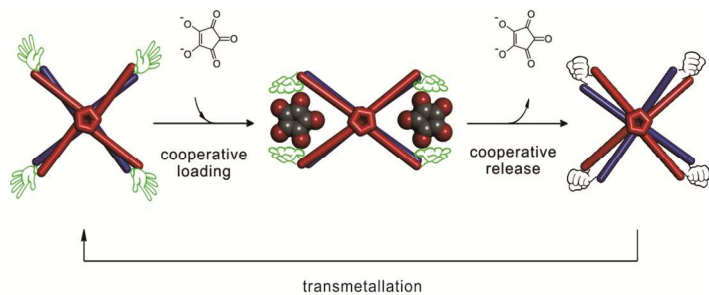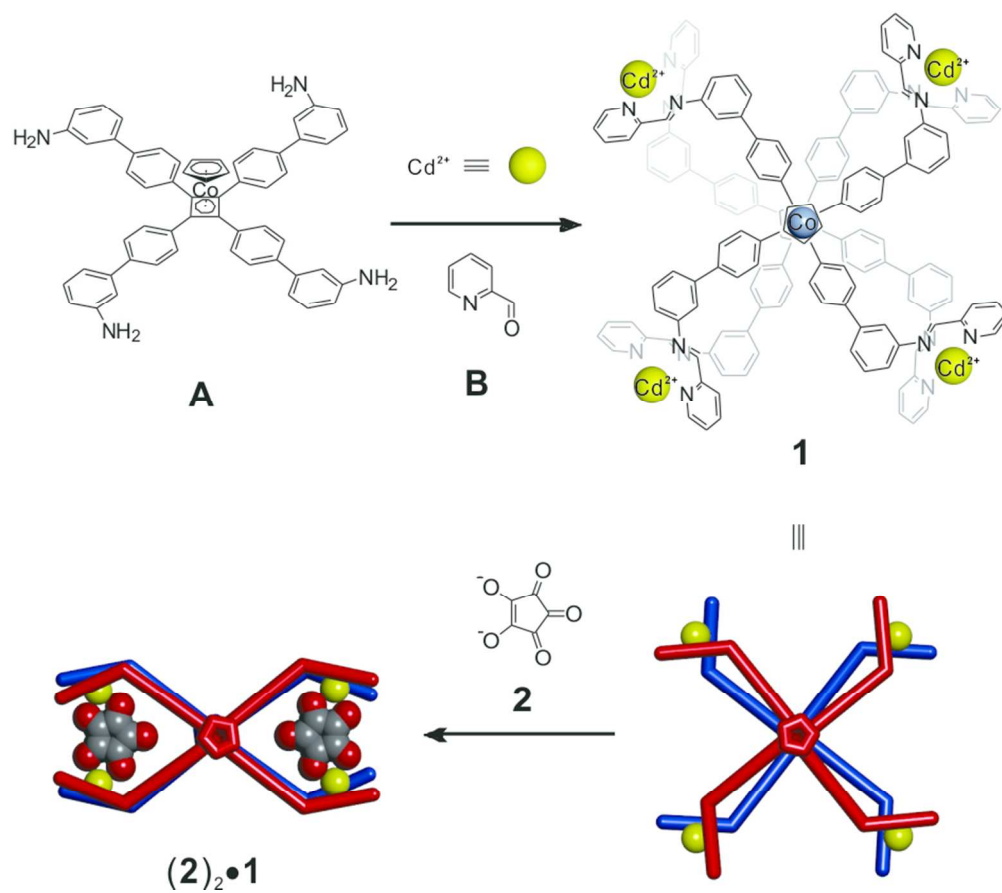
80x70mm (300 x 300 DPI)

80x99mm (300 x 300 DPI)

80x83mm (300 x 300 DPI)

Partial 1H NMR spectra (400 MHz, 298 K) of the catch and release of anions following the cycle of Figure 3. a) Receptor 1•(NTf2)8 (0.25 mM) with Cu+ (4 equiv.) in CD3CN (500 uL); b) addition of 2 (2.4 equiv.) to solution a; c) addition of DMSO-d6 (50 uL) to solution b; d) precipitate obtained from addition of diethyl ether to c following dissolution in CD3CN (500 uL); e) addition of Cd2+ (4 equiv.) to solution d. 80x65mm (300 x 300 DPI)